JCTC Journal of Chemical Theory and Computation

Interaction Analysis of the Native Structure of Prion Protein with Quantum Chemical Calculations

Takeshi Ishikawa[†,‡] and Kazuo Kuwata*[,†,‡]

Division of Prion Research, Center for Emerging Infectious Disease, Gifu University, 1-1 Yanagido, Gifu 501-1194, Japan, and CREST Project, Japan Science and Technology Agency, 4-1-8 Honcho, Kawaguchi, Saitama 332-0012, Japan

Received August 28, 2009

Abstract: We examined the solvent interaction and intramolecular interaction of the native structure of prion protein (PrP) using quantum chemical calculations based on the fragment molecular orbital (FMO) method. The influence due to the geometrical fluctuation was taken into account by performing calculations on forty different conformations. Each FMO calculation was carried out at the MP2 level of theory with the cc-pVDZ in which the resolution of the identity approximation was employed to reduce the computational cost. The solvent interaction energies obtained from the calculations provided information about the hydrophilicity of the three α-helices. We examined the roles of the charged residues in retaining the native structure of PrP with the calculated intramolecular interaction energies. The analysis, focused on van der Waals interaction, showed that the hydrophobic residues were important for the stability of the native structure. Our results were also discussed in relation to the identified pathogenetic mutations of prion diseases. Additionally, we examined the distribution of the calculated values with 40 structures, in which we demonstrated the influence of geometrical fluctuations on quantum chemical calculations.

1. Introduction

The abnormal scrapie form of prion protein (PrP), which is a conformational isoform of the cellular form, causes transmissible spongiform encephalopathies,[1−3] for example, scrapie, bovine spongiform encephalopathy, and Creutzfeldt−Jakob disease. In these prion diseases, the conformational conversion from the cellular form to the scrapie form is a key event. Researchers have elucidated the structure of the cellular form at atomic resolution with experimental measurements.[4−8] However, despite many studies utilizing both experimental and theoretical approaches, the mechanism of the pathogenetic conversion as well as the structure of the scrapie form remain unclear. Here, we consider that detailed information about the interaction responsible for retaining the high-order structure of the cellular form will be helpful for the examination of the mechanisms of prion diseases.

With the growth of computer technology, a number of theoretical studies of large molecules including biomolecular systems with quantum chemical calculations have been reported. For example, the molecular-orbital derived polarization (MP) model,[9] in which an effective Hamiltonian of a whole system was introduced to reduce a computational effort, was reported by Gao. This model was developed for Monte Carlo simulations or molecular dynamics simulations of liquid−water systems with semiempirical quantum chemical methods. He performed statistical mechanical Monte Carlo simulations of a cubic box containing 267 water molecules, and averaging over millions of configurations was carried out.[10] If we focus our attention on ab initio quantum chemical methods, the fragment molecular orbital (FMO) method[11−13] is one of the most efficient approaches for calculations of large molecules. Some methodological concepts of the FMO scheme are analogous to those of the MP

* Corresponding author e-mail: kuwata@gifu-u.ac.jp.
† Gifu University.
‡ Japan Science and Technology Agency.

10.1021/ct900456v © 2010 American Chemical Society
Published on Web 12/30/2009

model, but detailed descriptions about the difference between two methods are beyond the scope of this Article.

The FMO method is known to be a powerful tool for analyzing the interaction of biomolecular systems because inter fragment interaction energy (IFIE) or pair interaction energy (PIE) is clearly defined.[14] The intermolecular interactions of many proteins with small compounds or DNA bases were examined using the IFIE, providing some useful information for fundamental research and drug discovery.[15−24] However, the intramolecular interaction of proteins (i.e., the interactions between two residues) has not been extensively examined with the FMO method despite the fact that such interactions are significant for understanding the higher-order structures of proteins. As one of a few examples, Kurisaki et al. developed a visualization method for the IFIEs, including the intramolecular interaction of a protein,[25] wherein the secondary structures of proteins were discussed with the matrix representation of the IFIEs.

The interaction of amino acid residues with the surrounding solvent molecules is also significant for retaining the native structures of proteins. In the previous studies with the FMO scheme, the solvent effect could be included using the two solvent models: the polarizable continuum model (PCM)[26] and the explicit solvent model.[27,28] We believe that the explicit solvent model is better than the PCM for the examination of the solvent interaction of the amino acid residues because not only electrostatic interactions but also charge transfer interactions can be included.

In most previous studies using the FMO method, researchers examined biomolecular systems using the results of a single structure (or a very few structures). However, a number of structures should be considered because proteins and solvent molecules have a significant geometrical fluctuation at body temperature. Very recently, Ishikawa et al. reported the FMO calculations using 20 different structures from the MD trajectory,[29] wherein they examined the influence of the geometrical fluctuation on the interaction energy between a protein and a small molecule. Their results indicated that the molecular interactions in biomolecular systems should be discussed using the averaged results of multiple structures.

In this work, we calculated the solvent interactions and intramolecular interactions of PrP with the FMO method. In these calculations, the solvent effect was included with the explicit solvent model, and the influence of the geometrical fluctuation was considered by performing multiple calculations with the different structures. Using our results, we will discuss the interactions retaining the native structure of PrP (i.e., the cellular form of PrP). In the following sections, we provide a brief description of the FMO method, and after presenting the computational details, we discuss the results of our calculations.

2. Method

2.1. Brief Description of the FMO Method. In the FMO method, a target molecule is divided into small fragments[11] by cutting C−C single bonds with projection operators.[12] The total energy is evaluated using the results of individual calculations of the fragments (referred to as monomers) and pairs of the fragments (referred to as dimers) with the following equation:[11]

$$E_{\text{total}} = \sum_{I<J} E_{IJ} - (N_{\text{f}} - 2)\sum_{I} E_I \tag{1}$$

where E_I and E_{IJ} are energies obtained from the monomer and the dimer calculations, respectively, and N_{f} is the number of fragments. In such calculations, the electrostatic potential from the other fragments, which is generally referred to as the environmental electrostatic potential (ESP), is included.[11,14] At the HF level of theory, the total energy can be rewritten as:

$$E_{\text{total}}^{\text{HF}} = \sum_{I} E'^{\text{HF}}_{I} + \sum_{I>J} \Delta E_{IJ}^{\text{HF}} \tag{2}$$

where E'^{HF}_I is the monomer energy without the ESP. Thus, one can consider that $\Delta E_{IJ}^{\text{HF}}$ is the interaction energy between two fragments.[14] This value is the IFIE or PIE, the formulation of which can be found in a previous paper.[14]

As is generally known, electrostatic interactions and charge transfer interactions are included in HF calculations, but van der Waals interactions or dispersion interactions are not. Therefore, the MP2 calculation should additionally be performed to evaluate the van der Waals interactions. In such cases, the total energy is corrected using the MP2 results according to the following equations:

$$E_{\text{total}}^{\text{MP2}} = E_{\text{total}}^{\text{HF}} + (\sum_{I} E_I^{\text{corr}} + \sum_{I>J} \Delta E_{IJ}^{\text{corr}}) \tag{3}$$

$$\Delta E_{IJ}^{\text{corr}} = E_{IJ}^{\text{corr}} - E_I^{\text{corr}} - E_J^{\text{corr}} \tag{4}$$

where E_I^{corr}, E_{IJ}^{corr}, and $\Delta E_{IJ}^{\text{corr}}$ are van der Waals contributions to the monomer energy, the dimer energy, and the IFIE, respectively.[30−32] Thus, the IFIE corrected with the MP2 method is

$$\Delta E_{IJ}^{\text{MP2}} = \Delta E_{IJ}^{\text{HF}} + \Delta E_{IJ}^{\text{corr}} \tag{5}$$

This equation clearly shows that one can obtain the interaction energies divided into two contributions, that is, $\Delta E_{IJ}^{\text{HF}}$ (electrostatic interactions and charge transfer interactions) and $\Delta E_{IJ}^{\text{corr}}$ (van der Waals interactions).

2.2. Interaction Analysis. In FMO calculations of typical biomolecular systems, amino acid residues and solvent molecules are basically treated as a single fragment. Thus, the interaction energy between a specific residue (assigned to fragment I) and all solvent molecules can be calculated as:

$$\Delta E_I^{\text{solvent}} = \sum_{J\in \text{solvent}} \Delta E_{IJ}^{\text{MP2}} \tag{6}$$

where the summation runs over the fragments assigned to the solvent molecules. The total interaction energy of the protein with the solvent molecules is obtained as:

$$\Delta E_{\text{total}}^{\text{solvent}} = \sum_{I\in \text{protein}} \Delta E_I^{\text{solvent}} \tag{7}$$

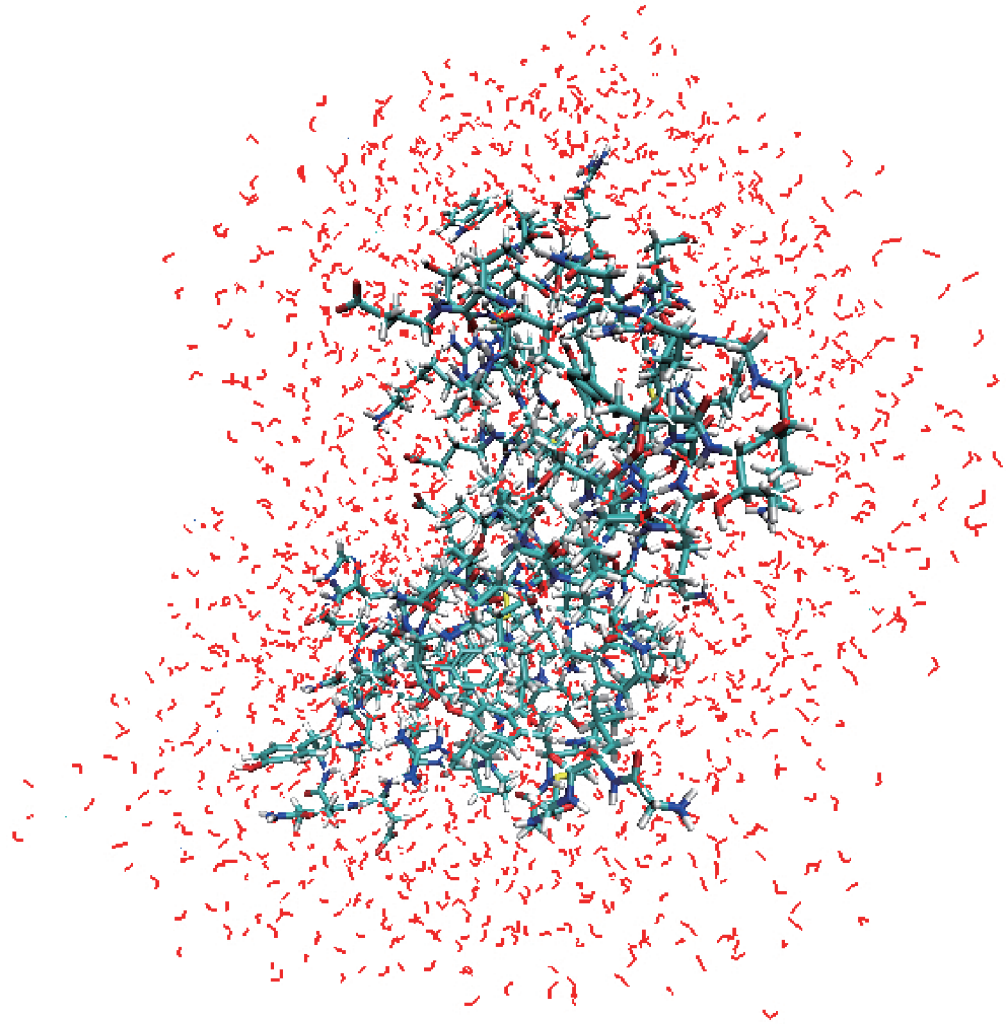

Figure 1. Graphical representation of our system. In this work, the FMO calculations were performed with the 40 different structures (see text).

where the summation runs over the fragments assigned to the protein. In a similar way, the interaction energies between two residues are obtained from $\Delta E_{IJ}^{\mathrm{MP2}}$. However, the interaction energies between two fragments connected to each other are not calculated because of the theoretical requirements of the FMO method. Thus, we cannot obtain the interaction energies between two neighboring residues.

Because the $\Delta E_{IJ}^{\mathrm{MP2}}$ is calculated with eq 5, the above interaction energies can be divided into the two contributions ($\Delta E_{IJ}^{\mathrm{HF}}$ and $\Delta E_{IJ}^{\mathrm{corr}}$). If these values are calculated in the native structure, we can obtain detailed information about the interactions that retain this structure.

3. Computational Details

We believed that a single calculation with a specific structure, for example, the geometry optimized structure, is not sufficient for the examination of biomolecular systems that have a geometrical fluctuation at a physiological temperature. We expect that the effect of this fluctuation can be partially introduced into our analysis by taking the average over the results with a number of geometrical structures. Thus, 40 calculations with different structures were performed to obtain the averaged results in this study. These atomic coordinates were prepared according to the following method.

(1) We downloaded an initial structure of the globular domain of PrP containing the residues 124−226 from the Protein Data Bank[33] (PDB code: 1AG2[4]). We then generated the missing hydrogen atoms and the solvent molecules (water molecules, sodium ions, and chloride ions) around the PrP.

(2) After an energy minimization of this system, we performed a constant temperature and pressure (300 K and 1 atm) ensemble simulation for 2120 ps under the truncated octahedron boundary condition with FF03[34] and TIP3P[35] (AMBER 10 package[36]).

(3) Forty structures were randomly selected from the trajectory of the last 1000 ps.

(4) For each structure, we excluded all solvent molecules more than 8.0 Å from the PrP, resulting in approximately 1800 solvent molecules within our systems.

We affirmed the validity of the cutoff distance of the solvent molecules (8.0 Å) as shown in the following section. Figure 1 shows an example structure of our system. Because we extracted the atomic coordinates around the native

conformation, our analysis yielded information about the interactions responsible for the stability of the native structure of the PrP.

In our FMO calculations, each amino acid residue was treated as a single fragment, except for C179 and C214, which were united into one fragment because of their S−S bond. The solvent molecules were essentially assigned as a single fragment, but ions and their hydration water molecules were collected into one fragment, in which the water molecules within 2.5 Å of the ions were treated as hydration waters.

We performed FMO calculations employing cc-pVDZ[37] at the MP2 level of theory together with the HF level of theory, wherein the total number of basis sets was about 60 000. In the case of the MP2 calculations, we utilized the resolution of the identity (RI) approximation[38] to reduce the computational efforts with auxiliary basis sets.[39] The RI-MP2 method was very recently introduced into the FMO scheme,[40] affording an advantageous increase in computational efficiency. As a result, timing of one FMO calculation of our system was about 70 h with the eight cores (Xeon E5420) and 2.0 GB memory per core. All calculations with the FMO scheme were performed using the PAICS program[29] developed in our laboratory.

As mentioned above, the statistical mechanical Monte Carlo simulations of liquid water systems were carried out with semiempirical quantum chemical methods.[10] However, to the best of our knowledge, this report is the first in which ab initio quantum chemical calculations of biomolecular systems including the explicit solvent molecules were carried out with 40 different structures.

4. Results and Discussion

4.1. MD Simulation. Prior to the discussions about the FMO calculations, we show the results of the MD simulation by which 40 structures used in our calculations were determined. This simulation was performed for 2120 ps with an energy minimized structure as an initial atomic coordinates. In this simulation, the atoms of PrP were restrained only for the first 20 ps, and, after that, this restraint was removed. The total energies of the system and the root-mean-square deviations (rmsd's) of the main-chains of PrP from the PDB structure are shown in Figure 2. Here, we selected the 40 structures from the trajectory of the last 1000 ps. In this range of the trajectory, the rmsd's were approximately 2.5−3.5 Å, indicating that a single structure calculation using the PDB structure is not sufficient for examinations of the native conformation of PrP.

4.2. Thickness of Solvent Molecules. As mentioned above, the explicit solvent molecules within 8.0 Å of the protein were included in our calculations to directly evaluate the interaction energies between residues and solvent molecules. Before starting the FMO calculations, we confirmed that the thickness of the solvent molecules was reasonable. The total solvent interaction energies ($\Delta E_{\mathrm{total}}^{\mathrm{solvent}}$) were calculated employing the various thicknesses. Figure 3 lists the results of calculations. In the case with a solvent molecule thickness of 12.0 Å, the interaction energy was −5204.9 kcal/mol. On the other hand, the interaction energy was −5091.4 kcal/mol for a 8.0 Å thickness, which was 97.8% of that with a 12.0 Å thickness. Judging from these calculations, we can safely say that our cutoff distance was reasonable for evaluating the interaction energies between residues and solvent molecules.

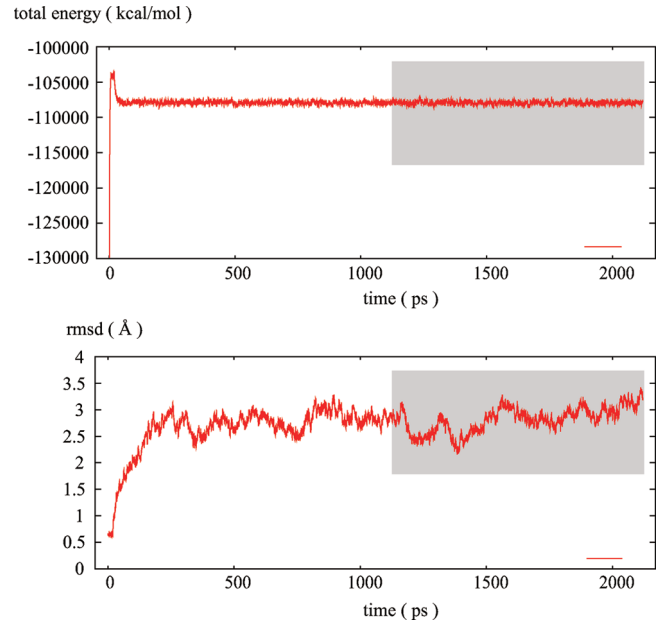

Figure 2. The total energy of the system and the rmsd of main-chains of PrP from the PDB structure. The shadow squares present the range from 1120 to 2120 ps, from which the 40 structures used for the FMO calculations were picked up.

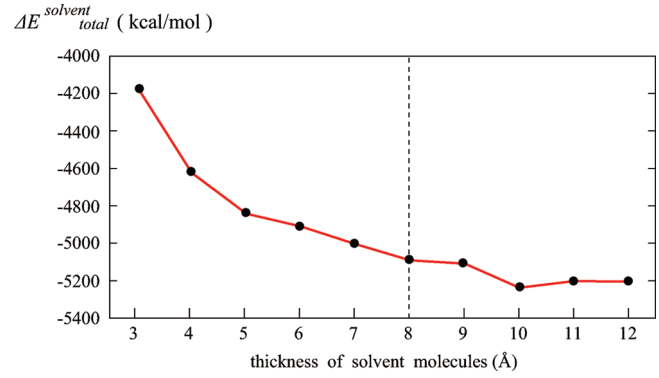

Figure 3. The total interaction energies between PrP and solvent molecules ($\Delta E_{\mathrm{total}}^{\mathrm{solvent}}$) with different thicknesses of the explicit solvent molecules from 3.0 to 12.0 Å.

4.3. Solvent Interactions of Residues. In this subsection, we will discuss the interaction between amino acid residues and solvent molecules. Figure 4 shows the calculated interaction energies of each residue ($\Delta E_I^{\mathrm{solvent}}$), in which we added the result of C214 to that of C179 because these residues were treated as a single fragment. All of the interaction energies were obtained by taking the average over the results of the 40 structures.

First, we should note that several charged residues largely interacted with the solvent molecules, that is, E152, D167, K185, K194, E200, E211, K220, and E221. Two terminal residues (G124 and Y226) also largely interacted with the

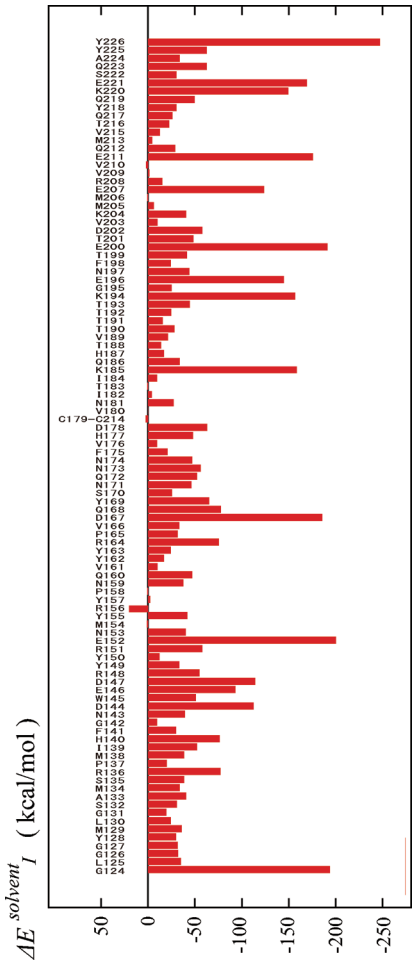

Figure 4. The interaction energies of residues with the solvent molecules ($\Delta E_I^{solvent}$). Because C179 and C214 were treated as a single fragment, the interaction energy of C214 was collected into C179. All of the interaction energies were obtained by taking the average from the 40 selected structures (see text).

solvent due to the setting of our calculation; that is, the main-chains of the two terminal residues were set to $-COO^-$ or $-NH_3^+$. These results are consistent with the common picture of proteins: hydrophilic residues tend to locate on the surface of a protein and interact with the surrounding solvent molecules, ensuring that these residues play important roles in retaining the native structure of the protein. However, our results indicated the existence of charged residues with comparatively small solvent interaction energies; particularly, R156 had an unfavorable interaction energy. In the next subsection, we will discuss the difference between two types of charged residues, that is, those having large solvent interaction energies and those having small solvent interaction energies.

The helical structures of PrP are known to decrease in the pathogenetic conversion of prion diseases,[41] but the broken parts of the helices have not been specified. Thus, the nature of each α-helix is important for studying the mechanism of prion diseases. The solvent interaction energies of the three α-helices can be obtained by restricting the summation of eq 7 to the fragments belonging to each helix according to the following equation:

$$\Delta E_{\text{helix}}^{\text{solvent}} = \sum_{I \in \text{helix}} \Delta E_I^{\text{solvent}} \tag{8}$$

where $\Delta E_I^{\text{solvent}}$ is defined in eq 6. Table 1 summarizes the calculated results. The solvent interaction energy per residue averaged within HA (D144−N153) was −76.9 kcal/mol. This result indicated that HA was highly hydrophilic. On the other hand, the averaged solvent interaction energy of HB (Q172−K194) was −38.7 kcal/mol, indicating low hydrophilicity. In the case of HC (E200−A224), the averaged solvent interaction energy was −53.6 kcal/mol. The high hydrophilicity of HA was previously pointed out by Morrissey and Shakhnovich,[42] who used the two empirical scaling criteria[43,44] for estimating the hydrophilicity.

From a methodological point of view, our scheme for evaluating the hydrophilicity of the secondary structures has notable points. For example, we evaluated the hydrophilicity from the direct calculations of the interaction energies with the solvent molecules in accordance with the quantum chemical calculations, in which not only electrostatic interactions but also charge transfer interactions can be included. Additionally, because the solvent interaction energies were individually calculated for each residue under the conditions of the protein, the hydrophilicity was evaluated reflecting the side-chain exposure to the solvent.

4.4. Ionic Interactions of Residues. In this subsection, we will discuss the intramolecular interactions of PrP. As mentioned above, we calculated the interaction energies between two non-neighboring residues. Figure 5 shows the results of the pairs having the 25 lowest interaction energies. At first glance, one should note that seven pairs have significantly larger interaction energies. Table 2 provides detailed information about these pairs. The seven pairs possessed ionic interactions; that is, two residues had electrically opposite charges and were separated by sufficiently small distance. Such ionic interactions are generally referred to as salt bridges. Here, we may consider that these seven salt bridges were one of the important sources causing the stability of the native conformation of PrP. These salt bridges might be inferred only with the structural information. However, we think that salt bridges can be identified more definitely by additional use of the energetic information.

Two salt bridges, D144−R148 and D147−R151, were located in HA with interaction energies of −119.6 and −98.7 kcal/mol, respectively. Thus, the helical structure of HA was strongly retained. Another salt bridge, K204−E207, was located in HC, and its interaction energy was −127.3 kcal/mol. This salt bridge contributed to the conservation of the helical structure of HC. On the other hand, there was no salt bridge in HB, indicating that the helical structure of HB was weaker than those of the other two helices. The remaining four salt bridges, R164−D178, R156−D202, E146−R208, and R156 −E196, were constructed with the two residues whose sequence numbers were separated from each other. This fact indicated that these four salt bridges were helpful in retaining the tertiary structure of the PrP. The ionic interaction is a local interaction between two specific residues, similar to that of a disulfide bond. Thus, we can consider that the native structure of the PrP is

Table 1. Solvent Interaction Energies of the Helices ($\Delta E_{helix}^{solvent}$) and the Whole Protein ($\Delta E_{total}^{solvent}$)[a]

$\Delta E_{helix}^{solvent}$			
HA	HB	HC	$\Delta E_{total}^{solvent}$
−769.0 (−76.9)	−850.8 (−38.7)	−1286.6 (−53.6)	−5077.2 (−49.3)

[a] The averaged interaction energies per residue are also shown in parentheses. These values are in kcal/mol. The interaction energies were obtained by taking the average from the 40 selected structures (see text).

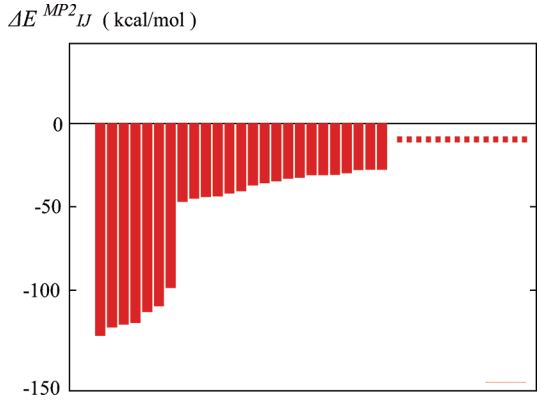

Figure 5. The 25 largest interaction energies of all of the pairs. Seven pairs had extremely large interaction energies as compared to the other pairs. These values were averaged results over the selected 40 calculations (see text).

Table 2. Interaction Energies of the Seven Pairs of Residues (kcal/mol)[a]

types of residues	energy	distance
K204−E207	−127.3	1.82
R164−D178*	−122.4	1.99
R156−D202*	−120.6	1.87
D144−R148*	−119.6	2.05
E146−R208*	−113.0	1.81
R156−E196*	−109.7	1.87
D147−R151	−98.7	2.38

[a] In this table, the sequence number of residues and the distance (Å) are also shown. These interaction energies were obtained by taking the average from the 40 selected structures (see text). The asterisk indicates that the pathogenetic point mutation involved with the pair has been identified.[45]

stabilized by several local interactions, that is, the seven salt bridges and one disulfide bond between C179 and C214.

Currently, researchers have identified a number of pathogenetic mutations of prion diseases.[45] Our results associated with the salt bridges were consistent with some of them. From the list of such pathogenetic mutations,[45] five point mutations are involved with the salt bridges, that is, R148H, D178N, E196K, D202N, and R208H. The ionic interaction of the salt bridge is eliminated by these mutations, and the native structure of PrP becomes destabilized. As a result, the pathogenetic conversion of prion diseases progresses. This consistency of our results with the pathogenetic mutations shows the potential of quantum chemical calculations in the ongoing studies of prion diseases.

Next, we discuss the ionic interactions in cooperation with the solvent interactions of the residues. In the range of the sequence numbers from 124 to 226, there are 22 charged

Table 3. Averaged Solvent Interaction Energy of Charged Residues Related to the Salt Bridges and Not Related to the Salt Bridges (kcal/mol)[a]

charged residues related to salt bridges	charged residues not related to salt bridges
−71.3	−162.1

[a] These interaction energies were obtained by taking the average from the 40 selected structures (see text).

amino acid residues. According to Table 2, 13 charged residues were related to the salt bridges, and, consequently, nine charged residues were not. Table 3 shows the solvent interaction energy per residue averaged within the 13 charged residues as well as that within the other nine charged residues. As shown in this table, the solvent interaction energies of the charged residues forming the salt bridges were significantly smaller than those of the other charged residues. Particularly, the solvent interaction energy of R156, which was related to the two salt bridges, was unfavorable. This result can be interpreted as follows. The location of the charged residue not related to the salt bridge can be adjusted to the interaction with the solvent molecules; that is, the side-chain is exposed to the solvent. On the other hand, the charged residue forming the salt bridge is located at a suitable position for an ionic interaction with the other charged residue. As a result, the location of their side-chains cannot be adjusted to interact with the solvent molecules. Here, we can state that the 13 charged residues play an important role for the stability of the protein by forming the salt bridges; on the other hand, the nine charged residues also play an important role by interacting with the solvent molecules. As shown in this subsection, our analysis provided information about the roles of the residues contributing to the stability of the native conformation of PrP.

4.5. van der Waals Interaction of Residues. In this subsection, we discuss the van der Waals interactions, which is the main source of the interactions between the hydrophobic residues. Here, to discuss the interactions retaining the high-order structure of PrP, we focus our attention on the interaction between two residues with sequence numbers separated from each other. Thus, we calculated the following values:

$$\Delta E_I^{vdw} = \sum_{J \in \text{protein}, |I-J|>5} \Delta E_{IJ}^{corr} \quad (9)$$

where ΔE_{IJ}^{corr} is van der Waals contribution to the interaction energy between the two fragments (see eq 5). The summation of J runs over the fragments whose index are different from I by more than five; that is to say, we accumulated the interaction energies between the residues separated from each other by more than five sequence numbers.

Figure 6 illustrates the calculated results. Phenylalanines and tyrosines, which have a benzene ring, showed large interaction energies associated with the van der Waals interaction. Additionally, several hydrophobic residues, leucine, methionine, valine, and isoleucine, had relatively large interaction energies, thus indicating that these residues contribute to the conservation of the native structure of PrP. These results are consistent with the common picture of

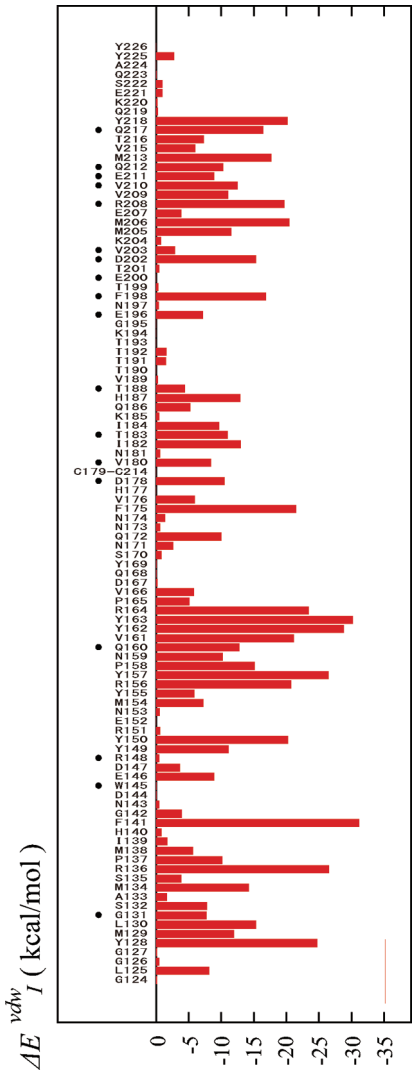

Figure 6. van der Waals interaction energies of each residue with the other residues separated by more than six sequence numbers (ΔE_I^{vdw}). Because C179 and C214 were treated as a single fragment, the interaction energy of C214 was collected into C179. These values were averaged results over the selected 40 calculations (see text). The dots over the residue name indicate that the pathogenetic point mutation of the residue has been identified.[45]

proteins: the side-chains of hydrophobic residues tend to be directed toward the inside of the protein and interact with the other hydrophobic residues, by which these residues play an important role in retaining the native conformation of the protein. Roughly speaking, in the case of PrP, several regions of the residues, Y128−F141, M154−V166, and M205−Y218, largely contribute to the retention of the native structure via van der Waals interactions. From the results in Figure 6, we can qualitatively say that van der Waals interaction is delocalized to many residues unlike the ionic interactions of the salt bridges. Several of the amino acid residues related to pathogenetic mutations[45] were labeled with black dots, some of which have large van der Waals interactions. Such results indicated a possibility that van der Waals interactions between residues may be important in the pathogenetic mechanism of prion diseases.

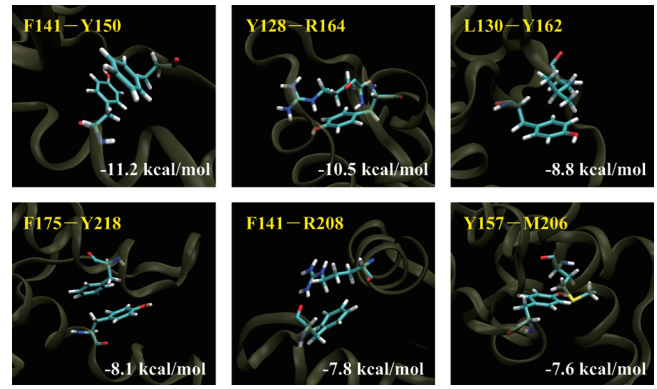

Figure 7. The six pairs of amino acid residues having the largest interaction energies associated with the van der Waals interaction (ΔE_{IJ}^{corr}). Two pairs had π/π type interactions, and four pairs had CH/π type interactions.

van der Waals interaction in biomolecular systems can be categorized as π/π interactions and CH/π interactions,[46] which are constructed from aromatic rings and C−H bonds. In recent years, such interactions have been considered to be important because many aromatic rings and C−H bonds exist in proteins. In Figure 7, we show the six pairs of amino acid residues with the largest van der Waals interaction energies in the PrP. Two pairs had π/π interactions (F141−Y150 and F175−Y218), and the other four pairs had CH/π interactions (Y128−R164, L130−Y162, F141−R208, and Y157−M206). Although only six pairs were illustrated in this Article, there are many pairs having such types of interactions. Therefore, π/π and CH/π interactions are considered to be important in retaining the high-order structure of the protein despite interaction energies smaller than those of the ionic interactions of the salt bridges.

4.6. Influence of Geometrical Fluctuation. Of theoretical interest, we discuss the influence of the geometrical fluctuation on the two quantities, that is, the solvent interaction energy of a protein ($\Delta E_{total}^{solvent}$) and the total energy of a protein ($E_{total}^{protein}$). The solvent interaction energy is defined in eq 7, and the total energy of protein can be calculated by restricting the summations of eq 3 within the fragments belonging to the protein.

Figure 8 illustrates the histograms of the 40 values obtained from calculations with the different structures. Although the rigorous discussion of the fluctuation is not possible here, we can roughly discuss the fluctuation of our results. In the case of the solvent interaction energy, the standard deviation and the difference between the maximum and minimum values were 142.5 and 507.0 kcal/mol, respectively. On the other hand, the standard deviation was 62.0 kcal/mol, and the difference between the maximum and minimum values was 233.1 kcal/mol in the total energy of the protein. The larger fluctuation of the solvent interaction energy reflected the high mobility of the solvent molecules. These results indicated that values obtained from the quantum chemical calculations for biomolecular systems might strongly depend on the selection of the atomic coordinates. Thus, we should always discuss the nature of proteins using averaged results with the various structure instead of one result with a single structure. Additionally, we intend to use our results

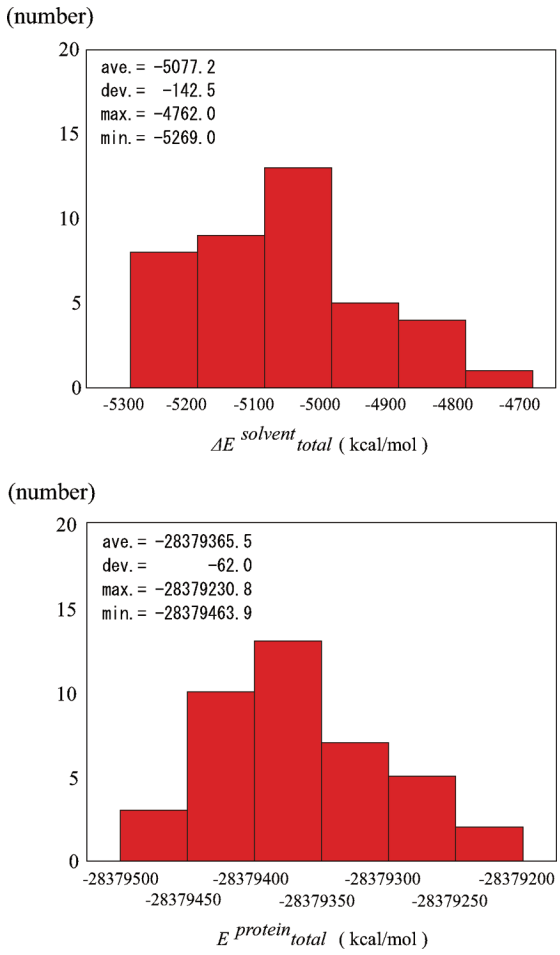

Figure 8. The two histograms of the energy distribution of the solvent interaction energy of the protein ($\Delta E_{total}^{solvent}$) and the total energy of the protein ($E_{total}^{protein}$). These data were obtained from the results using the selected 40 structures (see text). The average values, standard deviations, maximum values, and minimum values are also given.

in this subsection as fundamental data concerning the influence of the geometrical fluctuation of biomolecular systems in quantum chemical studies.

5. Summary

In this work, we examined the interactions retaining the native structures of PrP with quantum chemical calculations based on the FMO method. The solvent interactions could be included with the explicit solvent model, and the influence of the geometrical fluctuation was taken into account using the 40 results with different structures.

The direct calculation of the interaction energies between residues and solvent molecules showed that two types of charged residues exist, that is, those having large solvent interaction energies and those having small solvent interaction energies. The difference between them could be explained in connection with salt bridges. The calculated solvent interaction energy also revealed that HA had a high hydrophilicity while HB had a low hydrophilicity. Next, the intramolecular interaction energies provided information about the seven salt bridges of PrP. Two salt bridges, D144−R148 and E147−R151, contributed to retaining the helical structure of HA, and one salt bridge, K204−E207, stabilized the helical structure of HC. The remaining four salt bridges, R164−D178, R156−D202, E146−R208, and R156−E196, were helpful for conservation of the tertiary structure. These results about the salt bridges were consistent with some of the pathogenetic mutations of the prion diseases. Finally, we carried out the analysis of van der Waals interactions, which showed that several hydrophobic residues contributed to the stability of the native conformation. Our analysis indicated that several regions of the residues, Y128−F141, M154−V166, and M205−Y218, had large interaction energies associated with van der Waals interactions. It was also found that several residues related to the pathogenetic mutations had large van der Waals interactions, indicating an importance of van der Waals interactions in the pathogenetic mechanism. We expect that our results will be utilized in future studies to elucidate the mechanism of prion diseases.

From a theoretical point of view, we examined the influence of the geometrical fluctuation on the results of quantum chemical calculations. The standard deviation of the total energy and the solvent interaction energy were 62.0 and 142.5 kcal/mol, respectively. The larger fluctuation of the solvent interaction energy was considered to be caused by the high mobility of the solvent molecules. These results will be utilized as fundamental data concerning the influence of the geometrical fluctuation in ab initio quantum chemical studies for biomolecular systems.

Acknowledgment. This study was supported by a Grant-In-Aid for Young Scientist (Start-up) No. 20850020 from the Japan Society for the Promotion of Science. This study was also supported by the Program for Promotion of Fundamental Studies in Health Science of the National Institute of Biomedical Innovation. Calculations necessary in this study were performed using the computational resources at Gifu University.

References

(1) Prusiner, S. B. Novel proteinaceous infectious particles cause scrapie. *Science* **1982**, *216*, 136–144.

(2) Prusiner, S. B. Molecular biology and transgenetics of prion diseases. *Crit. Rev. Biochem. Mol. Biol.* **1991**, *26*, 397–438.

(3) Prusiner, S. B. Prions. *Proc. Natl. Acad. Sci. U.S.A.* **1998**, *95*, 13363–13383.

(4) Riek, R.; Hornemann, S.; Wider, G.; Billeter, M.; Glockshuber, R.; Wuthrich, K. NMR structure of the mouse prion protein domain PrP(121−231). *Nature* **1996**, *382*, 180–182.

(5) Donne, D. J.; Viles, J. H.; Groth, D.; Mehlhorn, I.; James, T. L.; Cohen, F. E.; Prusiner, S. B.; Wright, P. E.; Dyson, H. J. Structure of the recombinant full-length hamster prion protein PrP(29−231): The N terminus is highly flexible. *Proc. Natl. Acad. Sci. U.S.A.* **1997**, *94*, 13452–13457.

(6) James, T. L.; Liu, H.; Ulyanov, N. B.; Farr-Jones, S.; Zhang, H.; Donne, D. G.; Kaneko, K.; Groth, D.; Mehlhorn, I.; Prusiner, S. B.; Cohen, F. E. Solution structure of a 142-residue recombinant prion protein corresponding to the infectious fragment of the scrapie isoform. *Proc. Natl. Acad. Sci. U.S.A.* **1997**, *94*, 10086–10091.

(7) Gossert, A. D.; Bonjour, S.; Lysek, D. A.; Fiorito, F.; Wuthrich, K. Prion protein NMR structures of elk and of mouse/elk hybrids. *Proc. Natl. Acad. Sci. U.S.A.* **2005**, *102*, 646–650.

(8) Lysek, D. A.; Schorn, C.; Nivon, L. G.; Esteve-Moya, V.; Christen, B.; Calzolai, L.; von Schroetter, C.; Fiorito, F.; Herrmann, T.; Guntert, P.; Wuthrich, K. Prion protein NMR structures of cats, dogs, pigs, and sheep. *Proc. Natl. Acad. Sci. U.S.A.* **2005**, *102*, 640–645.

(9) Gao, J. Toward a molecular orbital derived empirical potential for liquid simulations. *J. Phys. Chem. B* **1997**, *101*, 657–663.

(10) Gao, J. A molecular-orbital derived polarization potential for liquid water. *J. Chem. Phys.* **1998**, *109*, 2346–2354.

(11) Kitaura, K.; Sawai, T.; Asada, T.; Nakano, T.; Uebayasi, M. Pair interaction molecular orbital method: an approximate computational method for molecular interactions. *Chem. Phys. Lett.* **1999**, *312*, 319–324.

(12) Kitaura, K.; Ikeo, E.; Asada, T.; Nakano, T.; Uebayasi, M. Fragment molecular orbital method: an approximate computational method for large molecules. *Chem. Phys. Lett.* **1999**, *313*, 701–706.

(13) Fedorov, D. G.; Kitaura, K. Extending the power of quantum chemistry to large systems with the fragment molecular orbital method. *J. Phys. Chem. A* **2007**, *111*, 6904–6914.

(14) Nakano, T.; Kaminuma, T.; Sato, T.; Fukuzawa, K.; Akiyama, Y.; Uebayasi, M.; Kitaura, K. Fragment molecular orbital method: use of approximate electrostatic potential. *Chem. Phys. Lett.* **2002**, *351*, 475–480.

(15) Fukuzawa, K.; Mochizuki, Y.; Tanaka, S.; Kitaura, K.; Nakano, T. Molecular interactions between estrogen receptor and its ligand studied by the ab initio fragment molecular orbital method. *J. Phys. Chem. B* **2006**, *110*, 16102–16110.

(16) Fukuzawa, K.; Komeiji, Y.; Mochizuki, Y.; Kato, A.; Nakano, T.; Tanaka, S. Intra- and intermolecular interactions between cyclic-AMP receptor protein and DNA: Ab initio fragment molecular orbital study. *J. Comput. Chem.* **2006**, *27*, 948–960.

(17) Ito, M.; Fukuzawa, K.; Mochizuki, Y.; Nakano, T.; Tanaka, S. Ab initio fragment molecular orbital study of molecular interactions between liganded retinoid X receptor and its coactivator: Roles of helix 12 in the coactivator binding mechanism. *J. Phys. Chem. B* **2007**, *111*, 3525–3533.

(18) Ito, M.; Fukuzawa, K.; Mochizuki, Y.; Nakano, T.; Tanaka, S. Ab initio fragment molecular orbital study of molecular interactions between liganded retinoid X receptor and its coactivator; Part II: Influence of mutations in transcriptional activation function 2 activating domain core on the molecular interactions. *J. Phys. Chem. A* **2008**, *112*, 1986–1998.

(19) Ito, M.; Fukuzawa, K.; Ishikawa, T.; Mochizuki, Y.; Nakano, T.; Tanaka, S. Ab initio fragment molecular orbital study of molecular interactions in liganded retinoid X receptor: Specification of residues associated with ligand inducible Iinformation transmission. *J. Phys. Chem. B* **2008**, *112*, 12081–12094.

(20) Amari, S.; Aizawa, M.; Zhang, J.; Fukuzawa, K.; Mochizuki, Y.; Iwasawa, Y.; Nakata, K.; Chuman, T.; Nakano, T. VISCANA: Visualized cluster analysis of protein−ligand interaction based on the ab initio fragment molecular orbital method for virtual ligand screening. *J. Chem. Inf. Model.* **2006**, *46*, 221–230.

(21) Nakanishi, Y.; Fedorov, D. G.; Kitaura, K. Molecular recognition mechanism of FK506 binding protein: An all-electron fragment molecular orbital study. *Proteins: Struct., Funct., Bioinf.* **2007**, *68*, 145–158.

(22) Iwata, T.; Fukuzawa, K.; Nakajima, K.; Aida, S. H.; Mochizuki, Y.; Watanabe, H.; Tanaka, S. Theoretical analysis of binding specificity of influenza viral hemagglutinin to avian and human receptors based on the fragment molecular orbital method. *Comput. Biol. Chem.* **2008**, *32*, 198–211.

(23) Ishikawa, T.; Mochizuki, Y.; Amari, S.; Nakano, T.; Tokiwa, H.; Tanaka, S.; Tanaka, K. Fragment interaction analysis based on local MP2. *Theor. Chem. Acc.* **2007**, *118*, 937–945.

(24) Ishikawa, T.; Mochizuki, Y.; Amari, S.; Nakano, T.; Tanaka, S.; Tanaka, K. An application of fragment interaction analysis based on local MP2. *Chem. Phys. Lett.* **2008**, *463*, 189–194.

(25) Kurisaki, I.; Fukuzawa, K.; Komeiji, Y.; Mochizuki, Y.; Nakano, T.; Imada, J.; Chmielewski, A.; Rothstein, S. M.; Watanabe, H.; Tanaka, S. Visualization analysis of interfragment interaction energies of CRP-cAMP-DNA complex based on the fragment molecular orbital method. *Biophys. Chem.* **2007**, *130*, 1–9.

(26) Fedorov, D. G.; Kitaura, K.; Li, H.; Jensen, J. H.; Gordon, M. S. The polarizable continuum model (PCM) interfaced with the fragment molecular orbital method (FMO). *J. Comput. Chem.* **2006**, *27*, 976–985.

(27) Komeiji, Y.; Ishida, T.; Fedorov, D. G.; Kitaura, K. Change in a protein's electronic structure induced by an explicit solvent: An ab initio fragment molecular orbital study of ubiquitin. *J. Comput. Chem.* **2007**, *28*, 1750–1762.

(28) Ishikawa, T.; Mochizuki, Y.; Nakano, T.; Amari, S.; Mori, H.; Honda, H.; Fujita, T.; Tokiwa, H.; Tanaka, S.; Komeiji, Y.; Fukuzawa, K.; Tanaka, K.; Miyoshi, E. Fragment molecular orbital calculations on large scale systems containing heavy metal atom. *Chem. Phys. Lett.* **2006**, *427*, 159–165.

(29) Ishikawa, T.; Ishikura, T.; Kuwata, K. Theoretical study of the prion protein based on the fragment molecular orbital method. *J. Comput. Chem.* **2009**, *30*, 2594–2601.

(30) Mochizuki, Y.; Nakano, T.; Koikegami, S.; Tanimori, S.; Abe, Y.; Nagashima, U.; Kitaura, K. A parallelized integral-direct second-order Møller-Plesset perturbation theory method with a fragment molecular orbital scheme. *Theor. Chem. Acc.* **2004**, *112*, 442–452.

(31) Mochizuki, Y.; Koikegami, S.; Nakano, T.; Amari, S.; Kitaura, K. Large scale MP2 calculations with fragment molecular orbital scheme. *Chem. Phys. Lett.* **2004**, *396*, 473–479.

(32) Fedorov, D. G.; Kitaura, K. Second order Møller-Plesset perturbation theory based upon the fragment molecular orbital method. *J. Chem. Phys.* **2004**, *121*, 2483–2490.

(33) Protein Data Bank (PDB); http://www.pdb.org/.

(34) Duan, Y.; Wu, C.; Chowdhury, S.; Lee, M. C.; Xiong, G.; Zhang, W.; Yang, R.; Cieplak, P.; Luo, R.; Lee, T. A point-charge force field for molecular mechanics simulations of proteins based on condensed-phase quantum mechanical calculations. *J. Comput. Chem.* **2003**, *24*, 1999–2012.

(35) Jorgensen, W. L.; Chandrasekhar, J.; Madura, J.; Klein, M. L. Comparison of simple potential functions for simulating liquid water. *J. Chem. Phys.* **1983**, *79*, 926–935.

(36) Case, D. A.; Darden, T. A.; Cheatham, T. E., III.; Simmerling, C. L.; Wang, J.; Duke, R. E.; Luo, R.; Crowley, M.; Walker, R. C.; Zhang, W.; Merz, K. M.; Wang, B.; Hayik, S.; Roitberg, A.; Seabra, G.; Kolossvàry, I.; Wong, K. F.; Paesani, F.;

Vanicek, J.; Wu, X.; Brozell, S. R.; Steinbrecher, T.; Gohlke, H.; Yang, L.; Tan, C.; Mongan, J.; Hornak, V.; Cui, G.; Mathews, D. H.; Seetin, M. G.; Sagui, C.; Babin, V.; Kollman, P. A. *AMBER 10*; University of California: San Francisco, CA, 2008.

(37) Dunning, T. H. Gaussian basis sets for use in correlated molecular calculations. I. The atoms boron through neon and hydrogen. *J. Chem. Phys.* **1989**, *90*, 1007–1023.

(38) Feyereisen, M.; Fitzgerald, G.; Komornicki, A. Use of approximate integrals in ab initio theory. An application in MP2 energy calculations. *Chem. Phys. Lett.* **1993**, *208*, 359–363.

(39) Weigend, F.; Köhn, A.; Hätting, C. Efficient use of the correlation consistent basis sets in resolution of the identity MP2 calculations. *J. Chem. Phys.* **2002**, *116*, 3175–3183.

(40) Ishikawa, T.; Kuwata, K. Fragment molecular orbital calculation using the RI-MP2 method. *Chem. Phys. Lett.* **2009**, *474*, 195–198.

(41) Nguyen, J.; Baldwin, M. A.; Cohen, F. E.; Prusiner, S. B. Prion protein peptides induce α-Hhelix to β-sheet conformational transitions. *Biochemistry* **1995**, *34*, 4186–4192.

(42) Morrissey, M. P.; Shakhnovich, E. I. Evidence for the role of PrPC helix 1 in the hydrophilic seeding of prion aggregates. *Proc. Natl. Acad. Sci. U.S.A.* **1999**, *96*, 11293–11298.

(43) Radzicka, A.; Wolfenden, R. Comparing the polarities of the amino acids: side-chain distribution coefficients between the vapor phase, cyclohexane, 1-octanol, and neutral aqueous solution. *Biochemistry* **1988**, *27*, 1664–1670.

(44) Kuhn, L. A.; Swanson, C. A.; Pique, M. E.; Tainer, J. A.; Getzoff, E. D. Atomic and residue hydrophilicity in the context of folded protein structures. *Proteins: Struct., Funct., Bioinf.* **1995**, *23*, 536–547.

(45) Kong, Q.; Surewicz, W. K.; Petersen, R. B.; Zou, W.; Chen, S. G.; Gambetti, P.; Parchi, P.; Capellari, S.; Goldfarb, L.; Montagna, P.; Lugaresi, E.; Piccardo, P.; Ghetti, B. In *Inherited Prion Diseases. Prion Biology and Diseases*, 2nd ed.; Prusiner, S. B., Ed.; Cold Spring Harbor Laboratory Press: New York, 2004; Chapter 14, pp 673−775.

(46) Nishio, M.; Hirota, M.; Umezawa, Y. *Specific Interactions in Protein Structures. The CH/π Interaction*; Wiley−VCH: New York, 1998; Chapter 11, pp 175−202.

CT900456V